EPJ Web of Conferences **49**, 15011 (2013)
DOI: 10.1051/epjconf/20134915011

Searches for pair production of third generation squarks with the ATLAS detector

Thomas Barber, on behalf of the ATLAS Collaboration[1]

[1] *Fakultät für Mathematik und Physik, Albert-Ludwigs-Universität, Freiburg, Germany*

Abstract. Naturalness arguments for weak-scale supersymmetry favour supersymmetric partners of the third generation quarks with masses not too far from those of their Standard Model counterparts. Production of third generation squarks via decay of a gluino can be significant if the mass of the gluino does not exceed the TeV scale. Scalar top or bottom squarks with masses less than a few hundred GeV can also give rise to direct pair production rates at the LHC that can be observed in the data sample recorded by the ATLAS detector. The talk presents recent ATLAS results from searches for gluino mediated and direct stop and sbottom pair production.

1 Introduction

Supersymmetry (SUSY) [1–9] is an extension of the Standard Model (SM) which naturally resolves the hierarchy problem by introducing supersymmetric partners to the known fermions and bosons. In the framework of a generic R-parity conserving minimal supersymmetric extension of the SM (MSSM) [10–14], SUSY particles are produced in pairs and the lightest supersymmetric particle (LSP) is stable. In a large variety of models the LSP is the lightest neutralino, $\tilde{\chi}_1^0$, which only interacts weakly. The scalar partners of right-handed and left-handed quarks (squarks) can mix to form two mass eigenstates ($\tilde{q}_1, \tilde{q}_2$). In particular, the third generation squarks (stop and sbottom, $\tilde{t}, \tilde{b}$), could have masses around the TeV scale.

In these proceedings, a summary of ATLAS searches for third generation squarks is presented, with emphasis on new results. The analyses are interpreted in a number of different simplified SUSY scenarios stemming from assumptions made regarding the mass spectrum.

If the stop and sbottom squarks are heavier than the gluino ($\tilde{g}$), indirect production is possible. The scenarios considered here additionally assume that the third generation squarks are also heavier than the neutralino, such that the reaction $pp \to \tilde{g}\tilde{g} \to t\bar{t}\tilde{\chi}_1^0 t\bar{t}\tilde{\chi}_1^0$, proceeds via an off-shell stop (known as the *Gtt* scenario). Similarly, the *Gbb* scenario allows the process $pp \to \tilde{g}\tilde{g} \to b\bar{b}\tilde{\chi}_1^0 b\bar{b}\tilde{\chi}_1^0$. Results are interpreted in this case in the $\tilde{\chi}_1^0 - \tilde{g}$ mass plane.

The cross section of direct production of third generation quarks is higher than the corresponding gluino-mediated cross section when mass of the squark is less than mass of the gluino. Four models of squark decay modes are considered. The sbottom can decay either via $\tilde{b} \to b\tilde{\chi}_1^0$ or $\tilde{b} \to t\tilde{\chi}_1^\pm$. For stop squarks, the decays $\tilde{t} \to t\tilde{\chi}_1^0$ or $\tilde{t} \to b\tilde{\chi}_1^\pm$ are assumed for heavy and light stops respectively. The decay $\tilde{t} \to c\tilde{\chi}_1^0$ is also considered as the subject of future ATLAS analyses and is not described here.

2 The ATLAS Detector

The ATLAS detector is described in detail elsewhere [15]. It comprises an inner detector (ID) surrounded by a 2 T superconducting solenoid, a calorimeter system and an extensive muon spectrometer embedded in a toroidal magnetic field. The ID tracking system consists of a silicon pixel detector, a silicon microstrip detector (SCT), and a transition radiation tracker (TRT). It provides tracking information for charged particles in a pseudorapidity[1] range $|\eta| < 2.5$ and allows efficient identification of jets originating from b-hadron decays. The ID is surrounded by high-granularity liquid-argon (LAr) sampling electromagnetic calorimeters. An iron/scintillator tile calorimeter provides hadronic energy measurements in the central pseudorapidity range ($|\eta| < 1.7$). In the forward regions ($1.5 < |\eta| < 4.9$), it is complemented by two end-cap calorimeters using LAr as the active material and copper or tungsten as an absorber. The muon spectrometer (MS) surrounds the calorimeters and consists of three large superconducting eight-coil toroids, a system of tracking chambers, and detectors for triggering.

3 General Analysis Description

The final states of third generation squark production are typically extremely rich, and can manifest themselves in a number of complementary channels. These include searches for events with leptons (electrons or muons), multiple jets (some of which may be b-tagged), and missing

[1] ATLAS uses a right-handed coordinate system with its origin at the nominal interaction point (IP) in the centre of the detector, with the z-axis coinciding with the beam pipe axis. The x-axis points from the IP to the centre of the LHC ring, and the y-axis points upwards. Cylindrical coordinates (r, ϕ) are used in the transverse plane, ϕ being the azimuthal angle around the beam pipe. The pseudorapidity is defined in terms of the polar angle θ as $\eta = -\ln\tan(\theta/2)$. The distance ΔR in the $\eta - \phi$ space is defined as $\Delta R = \sqrt{(\Delta\eta)^2 + (\Delta\phi)^2}$.

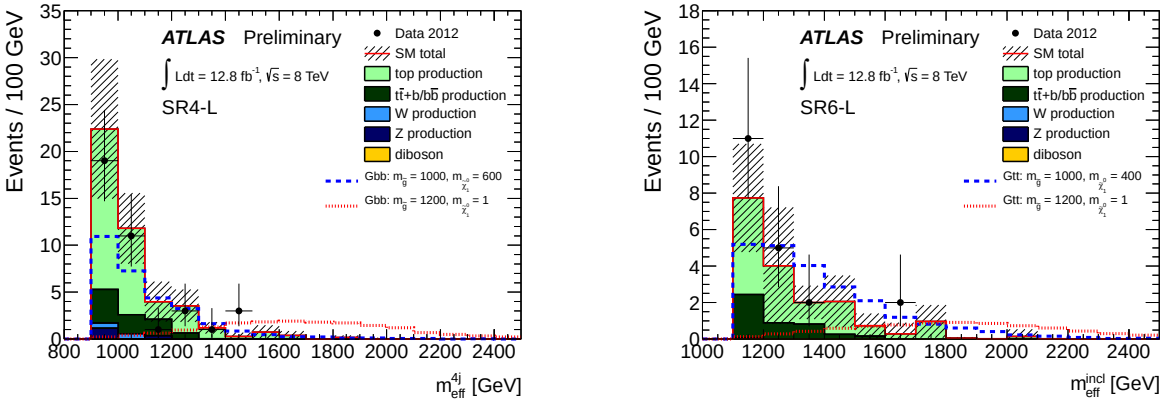

Figure 1. Distribution of the effective mass in the SR4-L (left) and SR6-L (right) signal regions, from Ref. [16]. The MC expectation is normalised to cross-section times integrated luminosity. The hatched band shows the statistical uncertainty on the simulated event samples combined with the detector related systematic uncertainty (among which jet energy scale and b-tagging uncertainties are dominant). The histogram labeled "top production" includes the contribution from $t\bar{t}$ +jets, $t\bar{t}$ + W/Z and single top production. Two signal points (with small and large mass splitting between the gluino and the LSP) for the *Gbb* and *Gtt* models are overlaid.

transverse energy. This section aims to give a general overview of how such events are reconstructed in ATLAS, which is broadly common across the analyses presented.

Electron candidates are reconstructed from energy clusters in the electromagnetic calorimeters matched to a track in the ID. They are required to have momentum in the transverse plane (p_{T}) above an analyses dependent threshold, $|\eta| < 2.47$ and to pass selection criteria of Ref. [17]. Muons are reconstructed using an algorithm [18] that combines information from the ID and MS. Candidate muons are required to have $|\eta| < 2.5$. Jet candidates are reconstructed using the anti-k_t jet clustering algorithm [19] with a radius parameter of $R = 0.4$. Only jet candidates with $|\eta| < 4.5$ are retained. A number of different b-tagging algorithms [20] are used to identify jets containing a b-hadron decay. The algorithms use multivariate techniques based on the properties of the secondary vertex, of tracks within the jet, and of the jet itself. The two-dimensional missing transverse momentum vector, $\mathbf{p}_{\mathrm{T}}^{\mathrm{miss}}$, and its magnitude $E_{\mathrm{T}}^{\mathrm{miss}}$, are computed from the negative of the vector sum of the p_{T} of the reconstructed electrons, photons, muons and jets, and all energy clusters with $|\eta| < 4.9$ not associated with such objects.

An analysis is typically performed by identifying a region of phase space where a particular signal is more prominent than the SM background. The backgrounds in question are estimated using a number of different methods. In some cases, such as multi-jet processes, the background can be estimated directly using fully data-driven methods [17, 21]. In other cases, for example many top pair production estimates ($t\bar{t}$), the background contribution is measured by normalising the Monte Carlo simulation to the number of data events in a dedicated control region which is rich in the background of interest. Other less significant backgrounds (for example diboson production) are taken directly from the Monte Carlo prediction.

In the case where no significant signal is observed, limits can be set on SUSY models. The numbers of predicted and measured events in each signal region are translated into 95% confidence-level (CL) upper limits on contributions from new physics using the CL_s prescription [22] with a profile log-likelihood ratio as a test statistic [23]. Some systematic uncertainties are not correlated between signal and backgrounds. However, the correlations between systematic uncertainties on the rates of signal and background events are taken into account.

4 Indirect Production Searches

One of the most sensitive analyses to the indirect production of sbottom and stop quarks specifically selects events with b-tagged jets. The analysis, described in detail in Ref. [16], is performed using 13 fb^{-1} of pp collision data at a centre-of-mass energy of $\sqrt{s} = 8$ TeV. Selection criterea require at least four jets with $p_{\mathrm{T}} > 50$ GeV, of which at least three must be b-tagged. The leading jet is required to have $p_{\mathrm{T}} > 90$ GeV, the event must have $E_{\mathrm{T}}^{\mathrm{miss}} > 200$ GeV and contain no lepton candidates. Two sets of signal regions are defined, one requiring at least four (SR4) and the other at least six (SR6) jets. SR4 is targeted more towards the *Gbb* scenarios, which contain four b-jets in the final state, while SR6 is more sensitive to the *Gtt* models. The main discriminating variable used for SR6 is the effective mass ($\mathrm{m_{eff}}$), defined as the scalar sum of the p_{T} of all jets in the event and the $E_{\mathrm{T}}^{\mathrm{miss}}$. Three signal regions are defined by requiring $\mathrm{m_{eff}} > 1100, 1300, 1500$ GeV and labelled L,M,T respectively. In SR4, a similar effective mass ($\mathrm{m_{eff}^{4j}}$) is defined from the scalar sum of the $E_{\mathrm{T}}^{\mathrm{miss}}$ and the leading four jets. Corresponding L,M,T regions require $\mathrm{m_{eff}^{4j}} > 900, 1100, 1300$ GeV. Distributions of $\mathrm{m_{eff}}$ and $\mathrm{m_{eff}^{4j}}$ are shown in Fig. 1. The dominant background contribution is from SM $t\bar{t}$ production in association with additional jets. This background is estimated by fitting the normalisation in a number of control regions. Other backgrounds including $t\bar{t}$ + $b/b\bar{b}$, W, Z and dibosons are estimated directly from simulations. As shown in Tab. 1,

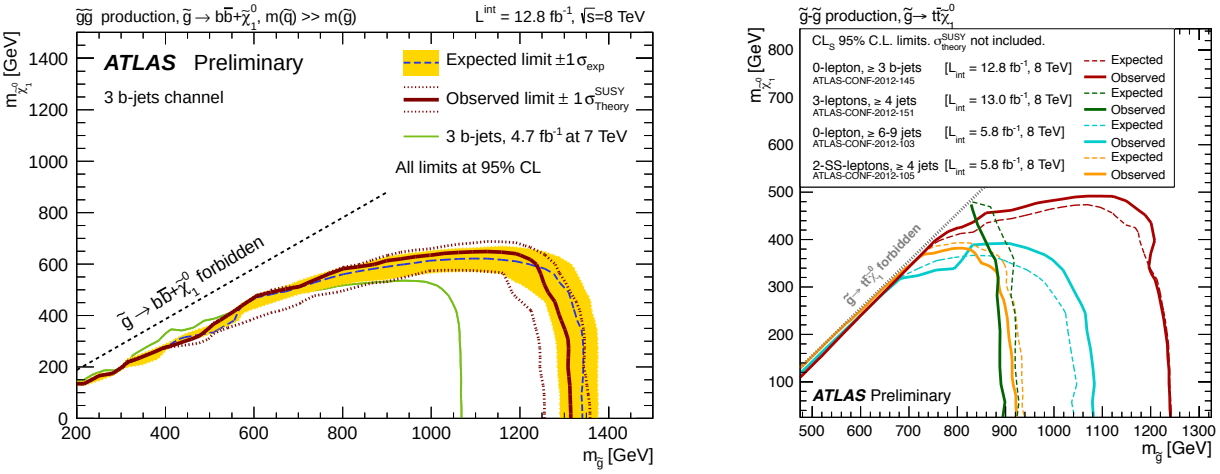

Figure 2. Exclusion contours in the $(m(\tilde{g}), m(\tilde{\chi}_1^0))$ plane for the *Gbb* model (left), from Ref. [24]. The dashed blue and solid bold red lines show the 95% CL expected and observed limits respectively, including all uncertainties except the theoretical signal cross-section uncertainty. The shaded (yellow) bands around the expected limits show the impact of the experimental uncertainties while the dotted red lines show the impact on the observed limit of the variation of the nominal signal cross-section by 1 sigma theoretical uncertainty. Also shown for reference are the results of the previous analysis. The right-hand plot (from Ref. [25]) shows exclusion contours at 95% CL for 8 TeV analyses in the $(m(\tilde{g}), m(\tilde{\chi}_1^0))$ plane for the *Gtt* simplified model where a pair of gluinos decays via off-shell stop to four top quarks and two neutralinos (LSP).

Table 1. The number of expected and observed events in each of the six signal regions in the b-jet analysis. The uncertainties on the expected number of events is a combination of systematic uncertainties and Monte Carlo statistics.

SR		L	M	T
4	Expected	46 ± 10	10.7 ± 2.9	2.9 ± 1.0
	Observed	38	8	4
6	Expected	18.1 ± 6.2	6.3 ± 2.4	2.2 ± 1.3
	Observed	20	4	2

the observed number of events is in good agreement with the SM expectation in all signal regions and the results are used to set limits on both models. As the signal regions are not exclusive, the region giving the best expected exclusion is chosen for each signal point, with the exclusion contours shown in Fig. 2. Assuming the central value of the SUSY cross section prediction (corresponding to the solid lines in Fig. 2), *Gbb* models with gluino masses below 1250 GeV are excluded for LSP masses below 200 GeV. In the corresponding *Gtt* case, gluinos lighter than 1240 GeV are excluded.

An analysis of final states with three leptons is also sensitive to the *Gtt* model [24]. The selection criteria require three leptons (e, μ) with a total charge of ±1 and $p_{\mathrm{T}} > 15$ GeV, with the leading lepton satisfying $p_{\mathrm{T}} > 20$ GeV. Events must also have at least four jets with $p_{\mathrm{T}} > 30$ GeV and $E_{\mathrm{T}}^{\mathrm{miss}} > 50$ GeV. A veto is applied to events with same-flavour, opposite-charge leptons having invariant mass $(m_{\ell\ell})$ between 81 GeV $< m_{\ell\ell} <$ 101 GeV to reject events containing Z boson decays. The dominant background in this analysis comes from events with two real leptons, and a third which is misidentified, for example $t\bar{t}$+ jets, WW+ jets and Z+ jets. The background contribution is determined using simulations, which are normalized with corrections factors derived from data. These correction factors depend on the charge and flavour combination of the leptons in the event, and are determined from data in six dedicated control regions. In total $9.7^{+3.8}_{-3.4}$ events are expected in 13 fb^{-1} of data at $\sqrt{s} = 8$ TeV, which is in good agreement with the 14 events observed. Limits are set on the *Gtt* scenarios, as shown in Fig. 2. Gluinos with masses lower than 900 GeV are excluded at 95% CL for a light neutralino, assuming the central value of the SUSY production cross section. This analysis also excludes compressed scenarios close to the kinematically forbidden region ($m_{\tilde{\chi}_1^0} \sim 450$ GeV, $m_{\tilde{g}} \sim 820$ GeV) where the b-jet analysis is not sensitive.

Results from two additional channels are used to set limits in the *Gtt* scenario. The first of these is a zero lepton, multi-jet analysis [26], which uses 5.8 fb^{-1} of data at $\sqrt{s} =$ 8 TeV. The second analysis requires two same-sign charge leptons and at least four jets using the same dataset [27]. The exclusion limits are shown in Fig. 2 alongside those of the previously described analyses.

5 Direct Sbottom Searches

The three lepton analysis in Sec. 4 is also used to set limits on direct sbottom pair production, via the decay channel $\tilde{b} \to t\tilde{\chi}_1^{\pm}$ followed by $\tilde{\chi}_1^{\pm} \to W^{\pm} + \tilde{\chi}_1^0$. Two scenarios are considered which make different assumptions about the mass relationship between the chargino and neutralino. In the first case, the assumption $m_{\tilde{\chi}_1^{\pm}} = 2 \times m_{\tilde{\chi}_1^0}$ is made, with limits set in the $\tilde{b} - \tilde{\chi}_1^0$ mass plane. Sbottom masses below 420 GeV are excluded for $m_{\tilde{\chi}_1^0} = 80$ GeV. In the second scenario, the neutralino mass is fixed to $m_{\tilde{\chi}_1^0} = 60$ GeV and limits are set in the $\tilde{b} - \tilde{\chi}_1^{\pm}$ mass plane. Sbottom masses

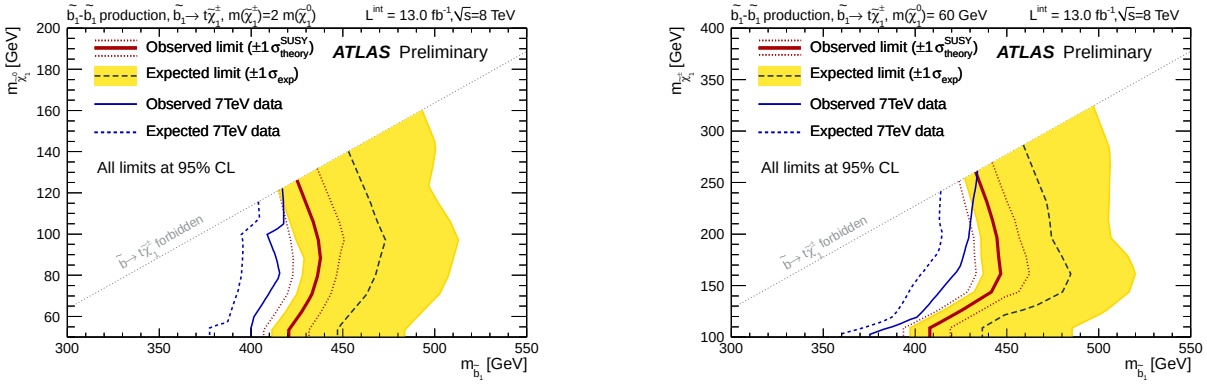

Figure 3. Expected and observed exclusion contour at 95% CL for direct sbottom production in the $m(\tilde{b} - \tilde{\chi}_1^0)$ (left) and $m(\tilde{b} - \tilde{\chi}_1^\pm)$ (right) planes, from Ref. [28].

of up to 430 GeV are excluded for chargino masses of 150 GeV to 210 GeV. The exclusion contours are shown in Fig. 3.

ATLAS has also performed a search for direct sbottom pair production in the $\tilde{b} \to b + \tilde{\chi}_1^0$ decay channel [28]. The latest iteration of the analysis uses 4.7 fb^{-1} of data at $\sqrt{s} = 7$ TeV, and selects events containing two b-tagged jets and large $E_{\mathrm{T}}^{\mathrm{miss}}$. Scalar bottom masses up to 490 GeV are excluded for $m_{\tilde{\chi}_1^0} = 0$ at 95% confidence level. Neutralino masses up to 180 GeV are excluded for scalar bottom masses around 400 GeV.

6 Direct Stop Searches

Direct stop production has been covered in ATLAS by five dedicated analyses using 4.7 fb^{-1} of data collected at 7 TeV, all of which set limits in the $\tilde{t} - \tilde{\chi}_1^0$ mass plane. For light stop masses ($m_{\tilde{t}} < 200$ GeV), the decay chain $\tilde{t} \to b + \tilde{\chi}_1^\pm$, followed by $\tilde{\chi}_1^\pm \to W + \tilde{\chi}_1^0$ is assumed, while $\tilde{t} \to t + \tilde{\chi}_1^0$ is assumed for higher masses.

In the light stop region, an analysis selecting events containing two soft leptons, large $E_{\mathrm{T}}^{\mathrm{miss}}$ and at least one jet is used to set limits assuming a fixed chargino mass of 106 GeV [29]. No excess of events is observed, allowing exclusion of stop masses up to 130 GeV for neutralino masses below 70 GeV. For stop squarks with masses similar to that of the top quark, an analysis [30] selecting events containing either one or two leptons, large $E_{\mathrm{T}}^{\mathrm{miss}}$ and b-tagged jets was used to set limits assuming $m_{\tilde{\chi}_1^\pm} = 2 \times m_{\tilde{\chi}_1^0}$ GeV. Light stop squarks with masses in the range 123-167 GeV are excluded for neutralino masses around 55 GeV.

In the higher mass range, three complementary analyses target the stop decay $\tilde{t} \to t + \tilde{\chi}_1^0$, based on final states containing zero, one or two leptons [31–33]. Overall, stop masses between $370 < m_{\tilde{t}} < 465$ GeV are excluded for $m_{\tilde{\chi}_1^0} \sim 0$ GeV. The full exclusion contour summarizing results from all of the direct stop searches is shown in Fig. 4.

7 Conclusions

ATLAS has a number of dedicated search channels sensitive to both indirect and direct production of third generation squarks. These proceedings give a summary of such searches, with emphasis on new results from an analysis based on final states containing multiple b-jets, and on a second containing three leptons. In both cases, no excesses over the SM expectations are observed, and exclusion limits are set on squark masses for the *Gbb*, *Gtt* and direct production models.

Searches for direct production of bottom and top squarks observe agreement between data and SM expectations. Consequently, ATLAS is continuing to extend exclusion limits across the wide range of searches for third generation squarks.

References

[1] H. Miyazawa, Prog. Theor. Phys. **36 (6)**, 1266 (1966)
[2] R. Ramond, Phys. Rev. **D3**, 2415 (1971)
[3] Y.A. Golfand, E.P. Likhtman, JETP Lett. **13**, 323 (1971), [Pisma Zh.Eksp.Teor.Fiz.13:452-455,1971]
[4] A. Neveu, J.H. Schwarz, Nucl. Phys. **B31**, 86 (1971)
[5] A. Neveu, J.H. Schwarz, Phys. Rev. **D4**, 1109 (1971)
[6] J. Gervais, B. Sakita, Nucl. Phys. **B34**, 632 (1971)
[7] D.V. Volkov, V.P. Akulov, Phys. Lett. **B46**, 109 (1973)
[8] J. Wess, B. Zumino, Phys. Lett. **B49**, 52 (1974)
[9] J. Wess, B. Zumino, Nucl. Phys. **B70**, 39 (1974)
[10] P. Fayet, Phys. Lett. **B64**, 159 (1976)
[11] P. Fayet, Phys. Lett. **B69**, 489 (1977)
[12] G.R. Farrar, P. Fayet, Phys. Lett. **B76**, 575 (1978)
[13] P. Fayet, Phys. Lett. **B84**, 416 (1979)
[14] S. Dimopoulos, H. Georgi, Nucl. Phys. **B193**, 150 (1981)
[15] ATLAS Collaboration, JINST **3**, S08003 (2008)
[16] ATLAS Collaboration, ATLAS-CONF-2012-145, `http://cdsweb.cern.ch/record/1493484`
[17] ATLAS Collaboration, Eur. Phys. J. **C72**, 1909 (2012)
[18] ATLAS Collaboration, ATLAS-CONF-2011-063, `https://cdsweb.cern.ch/record/1345743`
[19] M. Cacciari et al., JHEP **04**, 063 (2008)

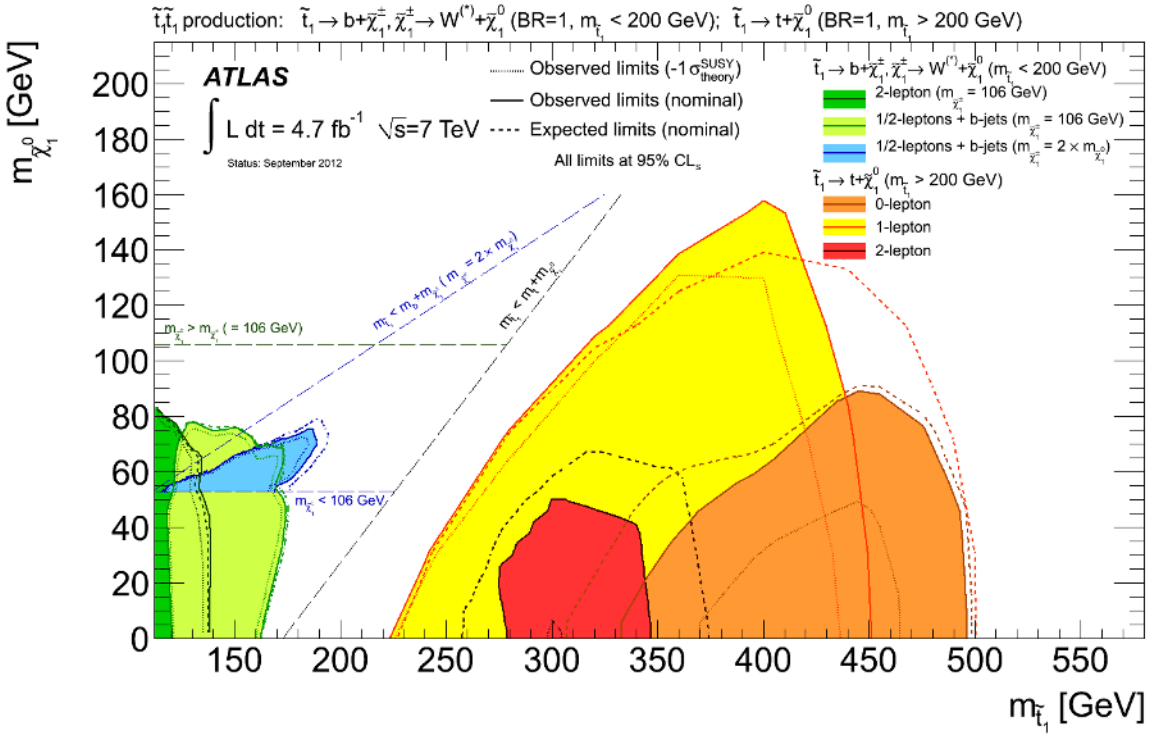

Figure 4. Summary of the five dedicated ATLAS searches for top squark (stop) pair production based on 4.7 fb^{-1} of pp collision data taken at $\sqrt{s} = 7TeV$, from Ref. [25]. Exclusion contours at 95% CL are shown in the $m(\tilde{t} - \tilde{\chi}_1^0)$ mass plane. The dashed and solid lines show the expected and observed limits, respectively, including all uncertainties except the theoretical signal cross section uncertainty (PDF and scale). The dotted lines represent the results obtained when reducing the nominal signal cross section by 1σ of its theoretical uncertainty. For stop masses below 200 GeV, the decay $\tilde{t} \to b + \tilde{\chi}_1^{\pm}, \tilde{\chi}_1^{\pm} \to W + \tilde{\chi}_1^0$ is assumed in all cases, with two hypotheses on the $\tilde{\chi}_1^{\pm}, \tilde{\chi}_1^0$ mass hierarchy, $m_{\tilde{\chi}_1^{\pm}} = 106$ GeV and $m_{\tilde{\chi}_1^{\pm}} = 2 \times m_{\tilde{\chi}_1^0}$ GeV. For stop masses above 200 GeV, the decay $\tilde{t} \to t + \tilde{\chi}_1^0$ is assumed to dominate.

[20] ATLAS Collaboration, ATLAS-CONF-2011-102, https://cdsweb.cern.ch/record/1369219

[21] ATLAS Collaboration, Phys. Lett. **B709**, 137 (2012)

[22] A.L. Read, J. Phys. **G28**, 2693 (2002)

[23] G. Cowan et al., Eur. Phys. J. **C71**, 1 (2011)

[24] ATLAS Collaboration, ATLAS-CONF-2012-151, http://cdsweb.cern.ch/record/1493490

[25] ATLAS SUSY results available at: https://twiki.cern.ch/twiki/bin/view/AtlasPublic/SupersymmetryPublicResults

[26] ATLAS Collaboration, ATLAS-CONF-2012-103, http://cdsweb.cern.ch/record/1472672

[27] ATLAS Collaboration, ATLAS-CONF-2012-105, http://cdsweb.cern.ch/record/1472674

[28] ATLAS Collaboration, ATLAS-CONF-2012-106, http://cdsweb.cern.ch/record/1472685

[29] ATLAS Collaboration, Eur. Phys. J. **C72**, 2237 (2012)

[30] ATLAS Collaboration (2012), arXiv:1209.2102 [hep-ex], Submitted to PLB

[31] ATLAS Collaboration (2012), arXiv:1208.1447 [hep-ex], Accepted by PRL

[32] ATLAS Collaboration, Phys. Rev. Lett. **109**, 211803 (2012)

[33] ATLAS Collaboration, JHEP **1211**, 094 (2012)